Neuroprotection by Δ^9-Tetrahydrocannabinol, the Main Active Compound in Marijuana, against Ouabain-Induced *In Vivo* Excitotoxicity

M. van der Stelt,[1] W. B. Veldhuis,[2,3] P. R. Bär,[3] G. A. Veldink,[1] J. F. G. Vliegenthart,[1] and K. Nicolay[2]

[1]*Department of Bio-Organic Chemistry, Bijvoet Center for Biomolecular Research, 3584 CH, Utrecht University, Utrecht, The Netherlands,* [2]*Department of Experimental In Vivo NMR, Image Sciences Institute, 3584 CJ, Utrecht, University Medical Center Utrecht, The Netherlands, and* [3]*Department of Experimental Neurology, University Medical Center Utrecht, 3584 CX, Utrecht, The Netherlands*

Excitotoxicity is a paradigm used to explain the biochemical events in both acute neuronal damage and in slowly progressive, neurodegenerative diseases. Here, we show in a longitudinal magnetic resonance imaging study that Δ^9-tetrahydrocannabinol (Δ^9-THC), the main active compound in marijuana, reduces neuronal injury in neonatal rats injected intracerebrally with the Na^+/K^+-ATPase inhibitor ouabain to elicit excitotoxicity. In the acute phase Δ^9-THC reduced the volume of cytotoxic edema by 22%. After 7 d, 36% less neuronal damage was observed in treated rats compared with control animals. Coadministration of the CB_1 cannabinoid receptor antagonist SR141716 prevented the neuroprotective actions of Δ^9-THC, indicating that Δ^9-THC afforded protection to neurons via the CB_1 receptor. In Δ^9-THC-treated rats the volume of astrogliotic tissue was 36% smaller. The CB_1 receptor antagonist did not block this effect. These results provide evidence that the cannabinoid system can serve to protect the brain against neurodegeneration.

Key words: anandamide; astrogliosis; cannabinoid; excitotoxicity; magnetic resonance imaging; neonatal rat; neuroprotection; ouabain; THC

The endogenous cannabinoid system comprises two cannabinoid receptors, designated CB_1 and CB_2, which have been cloned and characterized (Di Marzo, 1998). Two main endogenous ligands based on fatty acids, i.e., anandamide and 2-arachidonoylglycerol (2-AG) have been identified (Di Marzo, 1998). The CB_1 receptor is mainly found in the CNS, whereas the CB_2 receptor is almost exclusively expressed by cells of the immune system (Pertwee, 1997). The discovery of the endogenous cannabinoid system initiated intense research into the therapeutic potential of cannabinoids in a variety of neurological and neurodegenerative disorders, such as gliomas, cerebral ischemia, and multiple sclerosis (Nagayama et al., 1999; Baker et al., 2000; Galve-Roperh et al., 2000; Louw et al., 2000).

(Endo)cannabinoids have also been tested in models of excitotoxicity, which is a concept of neuronal cell death caused by overactivation of excitatory amino acid receptors. The excitotoxicity hypothesis is used to explain the common biochemical basis behind many acute and chronic neurodegenerative disorders such as stroke, traumatic brain injury, amyotrophic lateral sclerosis, Parkinson's, Huntington's, and Alzheimer's diseases (Dirnagl et al., 1999; Nicotera et al., 1999; Doble, 1999). *N*-acylethanolamines, including anandamide, and their precursors and 2-AG accumulate when tissues and cells are subjected to excitotoxic stress (Hansen et al., 1998, 2000; Di Marzo et al., 2000; Sugiura et al., 2000). Whether this increase in endocannabinoids is neuroprotective and if so via which mechanism is still under debate (Skaper et al., 1996a,b; Chan et al., 1998; Hampson et al., 1998; Shen and Thayer, 1998; Andersson et al., 2000; Sinor et al., 2000).

The therapeutic effects of cannabinoids in *in vivo* models of cerebral ischemia are also not consistent. Chronic Δ^9-THC administration has been shown to reduce the impact of an ischemic insult evoked by a reduced blood pressure and 12 min bilateral carotid artery occlusion. The involvement of the CB_1 receptor was not studied (Louw et al., 2000). However, no protective effect could be found for WIN55.212-2, a synthetic CB-receptor agonist, in rats when the middle cerebral artery was occluded for 2 hr. Surprisingly, the CB_1 receptor antagonist SR141716 was protective (C. J. Hillard, personal communication). Remarkably, WIN 55.212–2 afforded protection to hippocampal and cortical neurons in CB_1-dependent manner in rats with a permanent middle cerebral artery occlusion or global ischemia (Nagayama et al., 1999). The reason for this discrepancy is not known at the moment, but (endo)cannabinoid-induced vasorelaxation (Kunos et al., 2000) may have a different impact on the pathway of neuronal demise in each of these stroke models.

In light of the ambiguous results from both *in vitro* models of excitotoxicity and *in vivo* models of cerebral ischemia, we investigated the neuroprotective properties of Δ^9-THC in an *in vivo* model of secondary excitotoxicity. Neurodegeneration was elicited by inhibition of the Na^+/K^+-ATPase. Diffusion-weighted magnetic resonance imaging (MRI), T_2-weighted MRI, and histology, were used to study the effects of Δ^9-THC in both the acute and late phases after the induction of excitotoxicity.

Received March 22, 2001; revised May 31, 2001; accepted June 14, 2001.

W.B.V. is financially supported by the Netherlands Organization for Scientific Research, Medical Sciences Council. We are indebted to H. Veldman and G. van Haaften for expert technical assistance. Sanofi Recherche is gratefully acknowledged for the gift of SR141716. We thank Dr. R. Dijkhuizen for fruitful discussions and Dr. R. van Sluis for the development of the data analysis program.

M.vdS. and W.B.V. contributed equally to the work.

Correspondence should be addressed to G. A. Veldink, Department of Bio-organic Chemistry, Bijvoet Center for Biomolecular Research, Padualaan 8, 3584 CH, Utrecht University, Utrecht, The Netherlands. E-mail: veldink@accu.uu.nl.

Copyright © 2001 Society for Neuroscience 0270-6474/01/216475-05$15.00/0

MATERIALS AND METHODS

Animal model. Neonatal Wistar rats (U:Wu/Cpb; 7- to 8-d-old) were anesthetized with ether and immobilized in a stereotaxic frame. A small burr hole was drilled in the cranium over the left hemisphere, 2.5 mm lateral of bregma. A 1 μl syringe was lowered into the left striatum to a depth of 4.0 mm (Dijkhuizen et al., 1996). Ouabain (0.5 μl 1 mM; $n = 30$; Biomol, Zwijndrecht, The Netherlands) or vehicle (0.5 μl 40 mM Tris-HCl buffer, pH 7.4; $n = 2$) was injected at a rate of 0.125 μl/min with a microdrive. After injection the needle was left *in situ* for 2 min to avoid leakage of injection fluid from the needle tract. Animals were then positioned in the magnet, and anesthesia was continued with a mixture of halothane (0.4–1%) in N_2O/O_2. Body temperature was maintained at 37°C using a water-filled heating pad and an infrared heating lamp. Animals were treated with Δ^9-THC (Sigma Aldrich; $n = 12$), THC + SR141716 ($n = 5$; Sanofi Recherche, Montpellier, France), SR141716 ($n = 6$) (all drugs at 1 mg/kg in 1 ml/kg body weight 18:1:1 v/v PBS/Tween 80/Ethanol) 30 min before toxin injection. There was no difference in body weight and growth rate between any of the groups. The vehicle intraperitoneal injection did not affect lesion size. The University's Animal Experimental Committee approved all protocols.

MRI experiments. MRI was performed on a 4.7 T Varian horizontal bore spectrometer. Excitation and signal detection were accomplished by means of a Helmholtz volume coil (9 cm) and an inductively coupled surface coil (2 cm), respectively. A single-scan diffusion-trace MRI sequence [four *b* values:100–1300 sec/mm^2; repetition time (TR), 3 sec; echo time (TE), 100 msec] was used to generate quantified images of tissue water trace apparent diffusion coefficient (ADC). Diffusion trace- and T_2-weighted-imaging (TE, 18, 40, 62, and 84 msec; TR, 2 sec; number of transients, 2) were performed in all animals, starting at $t = 15$ min after injection on day 0 and were repeated 1 week later.

Both the T_2-weighted and the diffusion-weighted datasets consisted of seven consecutive, 1.5-mm-thick slices, with 0 mm slice gap. To minimize interference at the slice boundaries, slices were acquired in alternating order (1, 3, 5, 7, 2, 4, 6), thus maximizing the time between excitation of two neighboring slices. For the diffusion-weighted imaging we used a double spin-echo pulse sequence with four pairs of bipolar gradients with specific predetermined signs in each of the three orthogonal directions as recently published by De Graaf et al. (2001). The combination of gradient directions leads to cancellation of all off-diagonal tensor elements, effectively measuring the trace of the diffusion tensor. This provides unambiguous and rotationally invariant ADC values in one experiment, circumventing the need for three separate experiments. For each *b* value, two scans were averaged. The total scan time for acquisition of seven slices, with four *b* values and two averages, was 17 min.

As expected, at the early time point no changes in T_2-weighted MRI were detected. Animals not scanned at day 0 were kept under halothane anesthesia for equal durations as the scanned animals to prevent anesthesia-induced bias.

Data analysis. Monoexponential fitting using the Interactive Data Language software package generated ADC and T_2 maps. Parametric images were analyzed in anatomic regions of interest using Image Browser (Varian). Pixels in the ipsilateral hemisphere were considered pathological when their ADC or T_2 value differed more than twice the SD from the mean value in the contralateral hemisphere. The ventricles were segmented out in the average ADC and T_2 measurements. The lesion volume per slice was calculated by multiplying the lesion area (number of pathological pixels * field-of-view in cm^2/number of points acquired per image) by the slice thickness. The total lesion volume was obtained by summation of the lesion volumes for all slices. The absence of a slice gap makes interpolation of lesion areas between slices unnecessary, reducing systematic errors to within-slice "averaging" of signal intensity.

Statistical analysis was performed with SPSS 9.0. Differences between groups were analyzed using Student's *t* test; reported *p* values correspond to two-tailed significance.

Histology. After the last MRI measurements, animals needed for histology were transcardially perfused with 4% paraformaldehyde in 0.1 M PBS. Dissected brains were post-fixed overnight by immersion in the same fixative, cryoprotected in 10% sucrose in PBS for 24 hr, followed by 25% sucrose in PBS for 72 hr and quickly frozen in liquid nitrogen-cooled isopentane. We cut 10 μm coronal sections and stained them for glial fibrillary acidic protein (GFAP), Nissl substance, or hematoxylin–eosin with standard procedures. Position of the histological slices was matched to the position of MRI images by known position relative to bregma, after which a gross correlation was done.

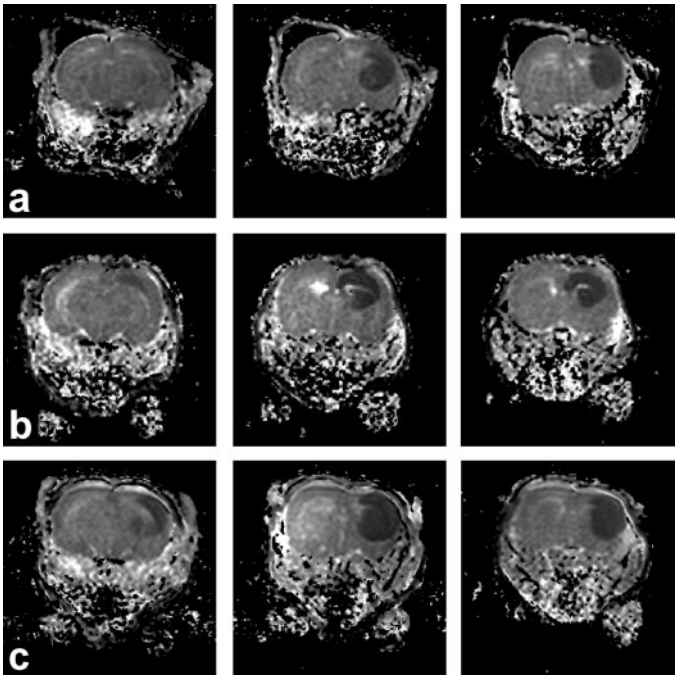

Figure 1. Three adjacent coronal ADC maps of neonatal rat brain 15 min after ouabain injection. *a,* No treatment; *b,* THC treatment; *c,* THC + SR141716 treatment. Hypointensities correlate to cytotoxic edema.

RESULTS

Loss of cellular ion homeostasis was initiated by unilateral intrastriatal injection of 0.5 μl of the Na^+/K^+-ATPase inhibitor ouabain (1 mM) into 7- to 8-d-old Wistar rats (Lees et al., 1990; Lees, 1991; Lees and Leong, 1995; Stelmashook et al., 1999). Twelve animals received an additional injection with Δ^9-THC (1 mg/kg, i.p.), and five animals received both Δ^9-THC and the CB_1 antagonist SR141716 (1 mg/kg, i.p.) 30 min before ouabain injection.

ADC maps of brain tissue water, calculated from diffusion-weighted MR images acquired 15 min after ouabain injection, showed hypointense regions with reduced ADC values ($\sim 0.67 \times 10^{-3}$ mm^2/sec) in the ipsilateral hemisphere in all animals (Fig. 1). Normal ADC values ($\sim 1.11 \times 10^{-3}$ mm^2/sec) were measured in the contralateral hemisphere of the ouabain-injected rats (Fig. 1) and in the brain of the control animals, which received only vehicle (0.5 μl Tris-HCl; 40 mM; pH 7.4). The reduction in ADC values in the ipsilateral hemispheres after ouabain injection is considered to reflect neuronal swelling, i.e., cytotoxic edema, because of a relocation of part of the extracellular water into depolarized cells (Van Lookeren Campagne et al., 1994; Dijkhuizen et al., 1996). In this acute phase, the volume of brain tissue with cytotoxic edema was 22% smaller in the Δ^9-THC group ($p < 0.05$) (Figs. 1, 2). Coinjection of the CB_1 receptor antagonist SR141716 completely abolished the Δ^9-THC-induced effect (Figs. 1, 2). The same brain regions, including the caudate putamen, cortex, and hippocampus, were affected in all animals (Fig. 1).

After 7 d, sharply delineated hyperintense regions were observed in the ADC maps (data not shown), indicative of the formation of vasogenic edema as well as tissue loss and ventricle dilatation. The volume of infarcted tissue as calculated from ADC maps was 36% smaller in Δ^9-THC-treated rats ($p < 0.01$) (Fig. 2). SR141716 abolished the protective effect ($p < 0.005$) (Fig. 2). An 18% increase in infarct volume was observed in the CB_1-

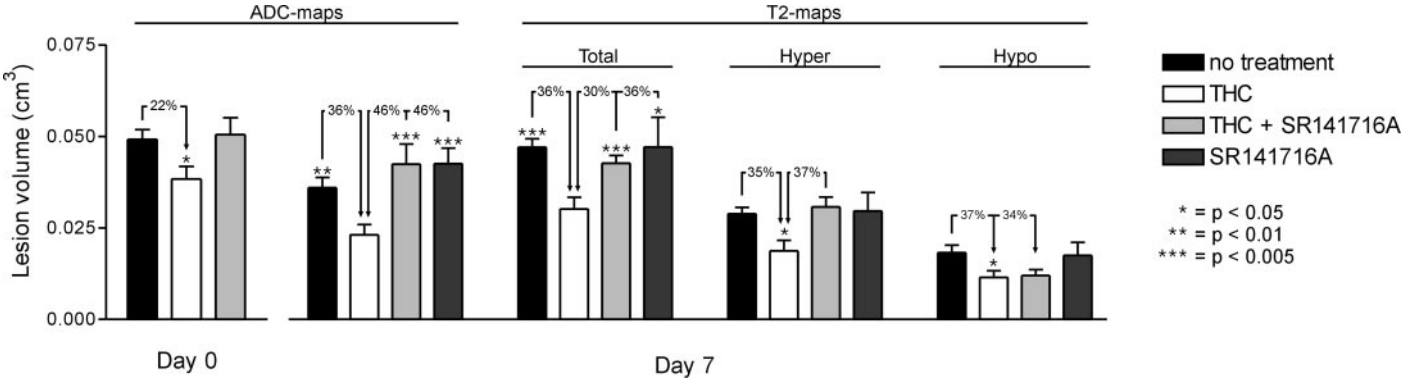

Figure 2. Mean lesion volumes (±SE) of ouabain-injected rats on days 0 and 7, based on ADC and T_2 map analysis.

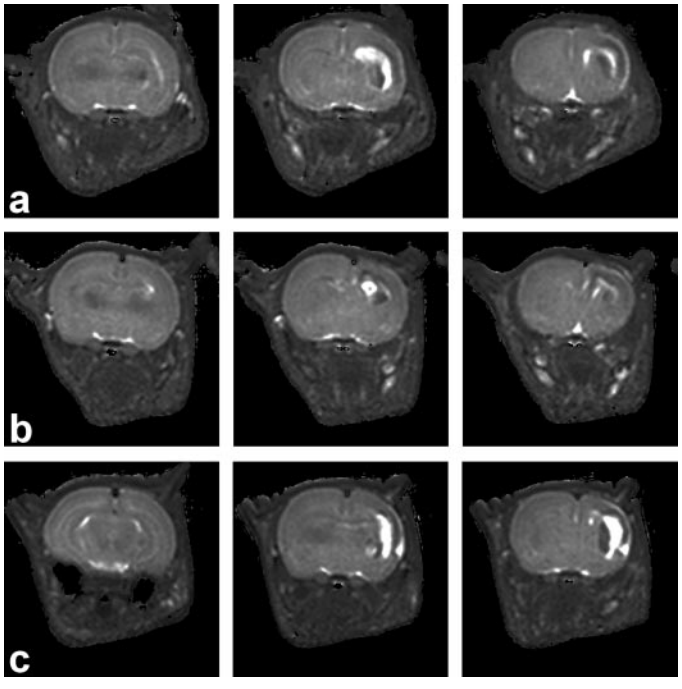

Figure 3. Three adjacent coronal T_2 maps of neonatal rat brain 7 d after ouabain injection. *a,* No treatment; *b,* THC treatment; *c,* THC + SR141716 treatment. Hyperintensities correlate to ventricle dilatation, vasogenic edema, and tissue loss, whereas hypointensities correlate to astrogliosis.

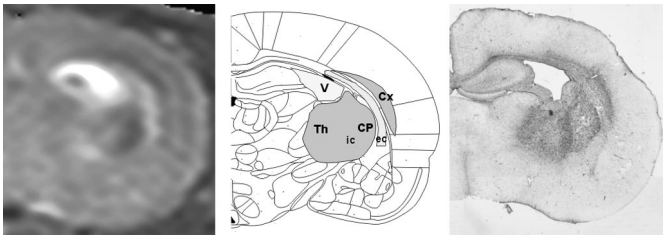

Figure 4. GFAP staining of a brain section of a ouabain-injected rat. Markedly increased staining was observed in the thalamus, external capsule, and cortex of the injected hemisphere, whereas normal staining was seen in the contralateral hemisphere.

antagonist-treated rats compared with nontreated rats (Fig. 2). This trend did not reach statistical significance. Neuroprotection was observed in brain regions known to express CB_1 receptors, such as the hippocampus, caudate putamen, and cortex (Fernandez-Ruiz et al., 2000). Western blot analysis confirmed the presence of CB_1-like receptors, but as expected, not of CB_2-like receptors, in 7- and 14-day-old rat brains (data not shown).

The effects of Δ^9-THC-treatment on neuronal damage after 7 d was also assessed using T_2-weighted imaging and verified with a histological procedure. T_2 maps demonstrated both hyperintensities and hypointensities (Fig. 3). Both types of T_2 abnormalities indicate pathological changes. Hyperintense areas correspond to vasogenic edema, tissue loss, and ventricle dilatation, whereas hypointensities correlate to astrogliosis, i.e., phenotypic changes (hypertrophy) and proliferation of astroglial cells in response to neuronal injury (Fig. 4) (Feuerstein et al., 1994; Van Lookeren Campagne et al., 1994). Lesion volumes, based on the combination of hyperintense and hypointense abnormalities on T_2 maps, were reduced by 36% ($p < 0.005$) in Δ^9-THC-treated rats compared with the control group (Figs. 2, 3). Infarct size based on T_2-hyperintense abnormalities was reduced by 35% in the Δ^9-THC-treated group ($p < 0.05$) compared with the control animals (Figs. 2, 3). This effect could be blocked by the CB_1 antagonist ($p < 0.05$) (Figs. 2, 3). Conventional histology (Nissl and hematoxylin–eosin staining) showed the same lesion pattern on brain sections and confirmed the assessment made by ADC and T_2 map analysis (data not shown).

The hypointense regions on the T_2 maps corresponded to regions exhibiting increased staining for GFAP staining, which is typical of astrogliosis, on brain sections of ouabain-treated rats (Fig. 4). No indications were found for hemorrhage. Astrogliotic tissue constituted 40% of the lesion on T_2 maps and usually surrounded the edematous tissue and the dilatated ventricles (Fig. 3). The volume of astrogliotic tissue in Δ^9-THC-treated rats was reduced by 37% compared with nontreated rats ($p < 0.05$). Importantly, this effect was not blocked by the CB_1 receptor antagonist (Fig. 2).

DISCUSSION

In the brain at least 40% of the energy produced by mitochondrial respiration is required by the Na^+/K^+-ATPase to maintain ion gradients across the cell membranes. Energy levels in the brain can be compromised by a lack of glucose and oxygen or by defects in the respiratory chain such as occurring in stroke and Parkinson's disease, respectively. Na^+/K^+-ATPase function is inhibited during energy failure. This may lead to a prolonged depolarization of the neuron, excessive release, and reversal of the uptake of excitatory amino acids, i.e., the induction of excitotoxicity (Dirnagl et al., 1999; Doble, 1999; Nicotera et al., 1999). Ouabain inhibits Na^+/K^+-ATPases and is a very potent neurotoxin that

leads to pancellular necrosis and infarction (Lees, 1991). It is used to study the involvement of Na^+/K^+-ATPase in CNS pathology (Lees et al., 1990; Lees, 1991; Lees and Leong, 1994, 1995; Stelmashook et al., 1999). Ouabain rapidly perturbs ion homeostasis and induces cell swelling and glutamate-dependent damage of cells, which can be prevented, at least in part, by blockade of the NMDA receptor (Lees et al., 1990; Lees, 1991; Lees and Leong, 1994, 1995; Cousin et al., 1995; Greene and Greenamyre, 1996; Basarsky et al., 1999; Buckley et al., 1999; Doble, 1999; Stelmashook et al., 1999).

The diffusion-weighted MRI data acquired 15 min after the injection of ouabain showed that activation of the CB_1 receptor by Δ^9-THC attenuates *in vivo* cell swelling in an early phase after the induction of excitotoxicity. Activation of the CB_1 receptor on presynaptic neuron terminals can lead to inhibition of the Ca^{2+} influx via N-, and P/Q-type voltage-sensitive calcium channels, thereby preventing the release of glutamate and subsequent depolarization of other neurons (Shen et al., 1996; Shen and Thayer, 1998). Furthermore, cannabinoids can induce hyperpolarization via the CB_1-mediated activation of inward rectifying and A-type K^+-channels (Deadwyler et al., 1993). Hyperpolarization raises the threshold to depolarization, which therefore may contribute to the observed reduction in the development of cytotoxic edema.

ADC and T_2 data acquired after 7 d demonstrated that Δ^9-THC or its CB_1-active metabolite 11-HO-Δ^9-THC reduced neuronal damage by 36%. Various mechanisms could underlie the following observed effects.

(1) Δ^9-THC-induced hypothermia (Pertwee, 1997). In our experimental setup, the body temperature of the rats was externally controlled by an infrared lamp and a water-heated pad, making the contribution of cannabinoid-induced hypothermia to the protective effects unlikely.

(2) Anti-oxidative properties of Δ^9-THC (Hampson et al., 1998). Anti-oxidant activity most likely does not play a major role in our model, because (1) the neuroprotective effects were blocked by the CB_1 antagonist, and (2) the dose of Δ^9-THC (1 mg/kg) is low compared with the high dose of anti-oxidant (50–100 mg/kg) required for effective protection in other studies (Hara et al., 1990),

(3) Downregulation of brain-resident mast cells by activation of a CB_2-like receptor (Skaper et al., 1996a,b). This process is also unlikely to be effective in our model, because (1) the neuroprotective effects were blocked by SR141716, (2) Δ^9-THC has been shown to have a low efficacy on the stimulation of the CB_2-receptor (Pertwee, 1997), and (3) a CB_2-like receptor could not be detected.

(4) Closing of N- and P/Q-type calcium channels via a CB_1-receptor-mediated mechanism (Shen and Thayer, 1996; Di Marzo et al., 1998). Reduced influx of calcium decreases directly the activation of destructive pathways, e.g., it prevents the activation of neuronal NO-synthase (Hillard et al., 1999) and it reduces glutamatergic transmission, i.e., induction of excitotoxicity (Shen et al., 1996; Shen and Thayer, 1998). This CB_1-mediated mechanism is likely to dominate the observed neuroprotective effects in the late phase in our model.

Neuroprotection by Δ^9-THC was observed in the hippocampus, striatum, and cortex. Western blots verified the presence of CB_1-receptors in neonatal rat brain. Previously, radioligand binding studies have demonstrated that CB receptors were expressed in the cerebral cortex, striatum, hippocampus, cerebellum, and brainstem at postnatal day 5 (Romero et al., 1997; Fernández-Ruiz et al., 2000). The presence of mRNA transcripts for the CB_1 receptor was also observed in some forebrain areas, such as the subventricular zone of the striatum, nucleus accumbens, and neocortex. The abundance of the mRNA transcripts was high at gestational day 21 but tended to wane to postnatal day 5 and disappeared at day 30 (Romero et al., 1997). Thus, these data support a CB_1-mediated neuroprotection.

The gliotic response to neuronal injury after ouabain injection has been reported in adult rats (Lees and Leong, 1995). We also observed astrogliosis surrounding vasogenic edema in our model. Δ^9-THC treatment reduced the volume of brain tissue with astrogliosis. Although astrocytes express CB_1-like receptors sensitive to SR141716 (Fernandez-Ruiz et al., 2000), administration of the SR141716 did not block the reduction in astrogliotic tissue. Therefore, this process does not seem to be mediated by a CB_1-like receptor. Noteworthy, dexanabinol, a nonpsychotropic cannabinoid, inhibits tumor necrosis factor-α (TNF-α) release from astrocytes (Shohami et al., 1997). It is thought that TNF-α sets the stage for inflammatory reactions including glial cell activation and proliferation (Feuerstein et al., 1994). Δ^9-THC is known to inhibit the release of TNF-α from immune cells (Klein et al., 1998). Thus, Δ^9-THC or one of its metabolites might also inhibit the release of TNF-α from astrocytes (or immune cells) and reduce astrogliosis. Furthermore, nonpsychotropic cannabinoid metabolites inhibit prostaglandin synthesis (Burstein, 1999). Cyclooxygenase-2 activation has been shown to induce astrogliosis (Brambilla et al., 1999). Thus, it is also possible that nonpsychotropic metabolites of Δ^9-THC reduce astrogliosis via this mechanism. Further research is required to investigate the mechanism of Δ^9-THC-induced reduction of astrogliosis.

Our data may suggest that endogenous cannabinoids could be released on neuronal injury and protect neurons in the periphery of the infarct: on the ADC maps we observed a trend toward a larger infarct (+18%) in antagonist-treated rats compared with nontreated rats (Figs. 2, 3). It should be noted that tissue was considered to be pathological only in case ADC or T_2 values differed more than twice the SD of the mean value in the contralateral hemisphere. The periphery of the infarct with smaller changes in ADC or T_2 is not incorporated in this way but may nevertheless have benefited from endogenous release of cannabinoids. Interestingly, the cortex was not severely damaged in the nontreated animals, whereas in the SR141716-injected animals this area was infarcted (Fig. 3*a*,*c*). It has been shown that glutamate-induced neurotoxicity leads to the formation of anandamide and its precursor *N*-acylphosphatidylethanolamine (Hansen et al., 1998, 2000). However, SR141716 is an inverse agonist. It is possible that SR141716 blocks constitutively active CB_1 receptors (Pertwee, 1997). Yet, Mechoulam and coworkers have found that the endogenous cannabinoid 2-AG is upregulated in the first hours after closed head injury in mice and that administration of 2-AG reduces edema formation via the CB_1 receptor, which strongly corroborates our findings (R. Mechoulam, personal communication).

In summary, we have shown that in an *in vivo* model of neurodegeneration Δ^9-THC reduces neuronal damage via a CB_1-receptor-mediated mechanism. This holds in both the acute and late phase after induction of excitotoxicity. Δ^9-THC inhibits astrogliosis via a non-CB_1-receptor-controlled mechanism. The results strengthen the concept that the endogenous cannabinoid system may serve to establish a defense system for the brain. This system may be functional in several neurodegenerative diseases in which excitotoxicity is thought to play a role, such as amyotrophic lateral sclerosis, Huntington's and Parkinson's diseases, and

also in acute neuronal damage as found in stroke and traumatic brain injury. It is conceivable that the endogenous cannabinoid system can be exploited for therapeutic interventions in these types of primarily incurable diseases.

REFERENCES

Andersson M, Jacobsson SO, Jonsson KO, Tiger G, Fowler CJ (2000) Neurotoxicity of glutamate in chick telencephalon neurons: reduction of toxicity by preincubation with carbachol, but not by the endogenous fatty acid amides anandamide and palmitoylethanolamide. Arch Toxicol 74:161–164.

Baker D, Pryce G, Croxford JL, Brown P, Pertwee RG, Huffman JW, Layward L (2000) Cannabinoids control spasticity and tremor in a multiple sclerosis model. Nature 404:84–87.

Basarsky TA, Feighan D, Mac Vicar BA (1999) Glutamate release through volume-activated channels during spreading depression. J Neurosci 19:6439–6445.

Brambilla R, Burnstock G, Bonazzi A, Ceruti S, Cattabeni F, Abbracchio MP (1999) Cyclo-oxygenase-2 mediates P2Y receptor-induced reactive astrogliosis. Br J Pharmacol 126:563–567.

Buckley DL, Bui JD, Phillips MI, Zelles T, Inglis BA, Plant HD, Blackband SJ (1999) The effect of ouabain on water diffusion in the rat hippocampal slice measured by high resolution NMR imaging. Magn Reson Med 41:137–142.

Burstein SH (1999) The cannabinoid acids: nonpsychoactive derivatives with therapeutic potential. Pharmacol Ther 82:87–96.

Chan GC, Hinds TR, Impey S, Storm DR (1998) Hippocampal neurotoxicity of Δ^9-tetrahydrocannabinol. J Neurosci 18:5322–5332.

Cousin MA, Nicholls DG, Pocock JM (1995) Modulation of ion gradients and glutamate release in cultured cerebellar granule cells by ouabain. J Neurochem 64:2097–2104.

Deadwyler SA, Hampson RE, Bennett BA, Edwards TA, Mu J, Pacheco MA, Ward SJ, Childers SR (1993) Cannabinoids modulate potassium current in cultured hippocampal neurons. Receptors Channels 1:121–134.

De Graaf RA, Braun KPJ, Nicolay K (2001) Single-shot Diffusion Trace 1H NMR Spectroscopy. Magn Reson Med 45:741–748.

Di Marzo V (1998) "Endocannabinoids" and other fatty acid derivatives with cannabimimetic properties: biochemistry and possible physiopathological relevance. Biochim Biophys Acta 1392:153–175

Di Marzo V, Hill MP, Bisogno T, Crossman AR, Brotchie JM (2000) Enhanced levels of endogenous cannabinoids in the globus pallidus are associated with a reduction in movement in an animal model of Parkinson's disease. FASEB J 14:1432–1438.

Di Marzo V, Melck D, Bisogno T, De Petrocellis L (1998) Endocannabinoids: endogenous cannabinoid receptor ligands with neuromodulatory action. Trends Neurosci 21:521–528.

Dijkhuizen RM, van Lookeren Campagne M, Niendorf T, Dreher W, van der Toorn A, Hoehn-Berlage M, Verheul HB, Tulleken CA, Leibfritz D, Hossmann KA, Nicolay K (1996) Status of the neonatal rat brain after NMDA-induced excitotoxic injury as measured by MRI, MRS and metabolic imaging. NMR Biomed 9:84–92.

Dirnagl U, Iadecola C, Moskowitz MA (1999) Pathobiology of ischaemic stroke: an integrated view. Trends Neurosci 22:391–397.

Doble A (1999) The role of excitotoxicity in neurodegenerative disease: implications for therapy. Pharmacol Ther 81:163–221.

Fernández-Ruiz J, Berrendero F, Hernandez ML, Ramos JA (2000) The endogenous cannabinoid system and brain development. Trends Neurosci 23:14–20.

Feuerstein GZ, Liu T, Barone FC (1994) Cytokines, inflammation, and brain injury: role of tumor necrosis factor-alpha. Cerebrovasc Brain Metab Rev 6:341–360.

Galve-Roperh I, Sanchez C, Cortes ML, del Pulgar TG, Izquierdo M, Guzman M (2000) Anti-tumoral action of cannabinoids: involvement of sustained ceramide accumulation and extracellular signal-regulated kinase activation. Nat Med 6:313–319.

Greene JG, Greenamyre JT (1996) Manipulation of membrane potential modulates malonate-induced striatal excitotoxicity in vivo. J Neurochem 66:637–643.

Hampson AJ, Grimaldi M, Axelrod J, Wink D (1998) Cannabidiol and (-)Δ^9-tetrahydrocannabinol are neuroprotective antioxidants. Proc Natl Acad Sci USA 95:8268–8273.

Hansen HS, Lauritzen L, Moesgaard B, Strand AM, Hansen HH (1998) Formation of *N*-acyl-phosphatidylethanolamines and *N*-acetylethanolamines: proposed role in neurotoxicity. Biochem Pharmacol 55:719–725.

Hansen HH, Hansen SH, Schousboe A, Hansen HS (2000) Determination of the phospholipid precursor of anandamide and other *N*-acylethanolamine phospholipids before and after sodium azide-induced toxicity in cultured neocortical neurons. J Neurochem 75:861–871.

Hara H, Kato H, Kogure K (1990) Protective effect of alpha-tocopherol on ischemic neuronal damage in the gerbil hippocampus. Brain Res 510:335–338.

Hillard CJ, Muthian S, Kearn CS (1999) Effects of CB(1) cannabinoid receptor activation on cerebellar granule cell nitric oxide synthase activity. FEBS Lett 459:277–281.

Klein TW, Friedman H, Specter S (1998) Marijuana, immunity and infection. J Neuroimmunol 83:102–115.

Kunos G, Jarai Z, Varga K, Liu J, Wang L, Wagner JA (2000) Cardiovascular effects of endocannabinoids–the plot thickens. Prostaglandins Other Lipid Mediat 61:71–84.

Lees GJ (1991) Inhibition of sodium-potassium-ATPase: a potentially ubiquitous mechanism contributing to central nervous system neuropathology. Brain Res Brain Res Rev 16:283–300.

Lees GJ, Lehmann A, Sandberg M, Hamberger A (1990) The neurotoxicity of ouabain, a sodium-potassium ATPase inhibitor, in the rat hippocampus. Neurosci Lett 120:159–162.

Lees GJ, Leong W (1994) Brain lesions induced by specific and non-specific inhibitors of sodium-potassium ATPase. Brain Res 649:225–233.

Lees GJ, Leong W (1995) The sodium-potassium ATPase inhibitor ouabain is neurotoxic in the rat substantia nigra and striatum. Neurosci Lett 188:113–116.

Louw DF, Yang FW, Sutherland GR (2000) The effect of Δ^9-tetrahydrocannabinol on forebrain ischemia in rat. Brain Res 857:183–187.

Nagayama T, Sinor AD, Simon RP, Chen J, Graham SH, Jin K, Greenberg DA (1999) Cannabinoids and neuroprotection in global and focal cerebral ischemia and in neuronal cultures. J Neurosci 19:2987–2995.

Nicotera P, Leist M, Manzo L (1999) Neuronal cell death: a demise with different shapes. Trends Pharmacol Sci 20:46–51.

Pertwee RG (1997) Pharmacology of cannabinoid CB_1 and CB_2 receptors. Pharmacol Ther 74:129–180.

Romero J, Garcia-Palomero E, Berrendero F, Garcia-Gil L, Hernandez ML, Ramos JA, Fernandez-Ruiz JJ (1997) Atypical location of cannabinoid receptors in white matter areas during rat brain development. Synapse 26:317–323

Shen M, Thayer SA (1998) Cannabinoid receptor agonists protect cultured rat hippocampal neurons from excitotoxicity. Mol Pharmacol 54:459–462.

Shen M, Piser TM, Seybold VS, Thayer SA (1996) Cannabinoid receptor agonists inhibit glutamatergic synaptic transmission in rat hippocampal cultures. J Neurosci 16:4322–4334.

Shohami E, Gallily R, Mechoulam R, Bass R, Ben-Hur T (1997) Cytokine production in the brain following closed head injury: dexanabinol (HU-211) is a novel TNF-alpha inhibitor and an effective neuroprotectant. J Neuroimmunol 72:169–177.

Sinor AD, Irvin SM, Greenberg DA (2000) Endocannabinoids protect cerebral cortical neurons from in vitro ischemia in rats. Neurosci Lett 278:157–160.

Skaper SD, Buriani A, Dal Toso R, Petrelli L, Romanello S, Facci L, Leon A (1996a) The ALIAmide palmitoylethanolamide and cannabinoids, but not anandamide, are protective in a delayed postglutamate paradigm of excitotoxic death in cerebellar granule neurons. Proc Natl Acad Sci USA 93:3984–3989.

Skaper SD, Facci L, Romanello S, Leon A (1996b) Mast cell activation causes delayed neurodegeneration in mixed hippocampal cultures via the nitric oxide pathway. J Neurochem 66:1157–1166.

Stelmashook EV, Weih M, Zorov D, Victorov I, Dirnagl U, Isaev N (1999) Short-term block of Na^+/K^+-ATPase in neuro-glial cell cultures of cerebellum induces glutamate dependent damage of granule cells. FEBS Lett 456:41–44.

Sugiura T, Yoshinaga N, Kondo S, Waku K, Ishima Y (2000) Generation of 2-arachidonoylglycerol, an endogenous cannabinoid receptor ligand, in picrotoxinin-administered rat brain. Biochem Biophys Res Commun 271:654–658.

Van Lookeren Campagne M, Verheul JB, Nicolay K, Balazs R (1994) Early evolution and recovery from excitotoxic injury in the neonatal rat brain: a study combining magnetic resonance imaging, electrical impedance, and histology. J Cereb Blood Flow Metab 14:1011–1023.